Archived in

dspace@nitr

http://dspace.nitrkl.ac.in/dspace

Published in Int J Adv Manuf Technol , Volume 34, Numbers 3-4 / September, 2007, P 227-235

http://dx.doi.org/10.1007/s00170-006-0589-0

S S Panda is presently with National Institute of Technology Rourkela

Email sudhansusekhar.panda@gmail.com

Monitoring of drill flank wear using fuzzy back propagation neural network

S. S. Panda, D. Chakraborty*,

Mechanical Engineering Department
Indian Institute of Technology Guwahati, Guwahati 781 039, India

and
S. K. Pal

Mechanical Engineering Department
Indian Institute of Technology Kharagpur, Kharagpur 721 302, India

Abstract

The present work deals with developing a fuzzy back propagation neural network scheme for prediction of drill wear. Drill wear is an important issue in the manufacturing industries, which not only affects the surface roughness of the hole but also influences the drill life. Therefore, replacement of drill at an appropriate time is of significant importance. Flank wear in a drill which depends upon the input parameters like, speed, feed rate, drill diameter, thrust force, torque and chip thickness. Therefore sometimes it becomes difficult to have a quantitative measurement of all the parameters and a qualitative description becomes easier. For this kind of situations, a fuzzy

back propagation neural network model has been trained in the present work and has been shown to predict drill wear with reasonable accuracy. In the present case a left and right (LR) type fuzzy neuron has been used. The proposed model is composed of various modules like fuzzy data collection at input fuzzy neuron, defuzzyfication of input data to get output, calculation of mean square error (MSE) and feeding back to update the network. Results from the present work show a very good prediction of drill wear from the present fuzzy back propagation neural network model.

Keywords: *Neuro-fuzzy system; LR type fuzzy neuron; Sensor signal; Flank wear*

* Corresponding author. Tel No.: +91-361-2582666; fax: +91-361-2690762

E-mail address: chakra@iitg.ernet.in

1 Introduction

In order to achieve improved productivity and better quality of the product in drilling operation, monitoring of drill wear is an important issue. Since drill wear affects the hole quality and tool life of the drill, online monitoring and prediction of drill wear is an important area of research. Many works have already been reported in the broad area of tool condition monitoring. Following paragraph describes some of the relevant research in this direction.

Lin and Ting [1] studied the effect of drill wear as well as other cutting parameters on the current force signals, and established the relationship between the force signals and drill wear with the other cutting parameters. In another work Lin and Ting [2] used the neural network model to study the drill wear. They observed that the training error in case of sample mode converges faster than that in case of batch mode. They also observed that the training error with two hidden layers converges faster than that with one hidden layer with same total processing element. Lee et al. [3] used the abductive network modeling in drilling process for predicting the drilling performance (tool life, thrust force and torque). In their work they used a network having number of polynomial functional nodes and the input to the network was drilling process parameters (speed, feed and diameter). Optimal network architecture was prepared based on predicted square error criterion. They used simulated annealing to optimize the process parameter. Xiaoli and Tso [4] monitored the tool wear based on current signals of spindle motor and feed motor using regression model. Tsao [5] used the radial basis function network (RBFN) and adaptive based radial basis function network (ARBFN) to predict the flank wear, and compared their results with experimental observation. Ertunc and Loparo [6] used decisions fusion center

algorithm (DFCA) for monitoring online tool wear condition in drilling process, and used number of numerical methods for predicting the condition of tool wear land. Abbu-Mahfouz [7] predicted wear rate in drilling using vibration signature analysis. He estimated three different patterns of vibration signatures like harmonic wavelets coefficient, power spectra density and Fast Fourier Transformation (FFT), and those vibration signature were used as inputs to the neural network model. Multiple objectives linear programming models for optimizing drill hole quality with different cutting conditions such as speed and feed rate was proposed by Kim and Ramulu [8]. Singh et al. [9] used back propagation neural network for prediction of flank wear of HSS drill in a copper work piece. They used spindle speed, feed rate, drill diameter, thrust force and torque as input parameters and maximum flank wear as output parameter to neural network. Li et al. [10] proposed hybrid learning for monitoring of drill wear using a combination of fuzzy system and neural network. Kuo and Kohen [11] applied a modified fuzzy neural network for detecting the defective sensor signal using membership function at the input node and fuzzy rule base. Lo [12] described the tool state in turning operation using artificial neuro fuzzy inference system (ANFIS) architecture, and concluded that higher accuracy could be achieved in the case of triangular and bell shape membership function. Hashmi et al. [13] proposed a fuzzy model for correlating the drilling speed with hardness of work material. They have used triangular membership function with fuzzy rule base in there analysis.

Literature review reveals that a number of works have been reported in the subject of drill wear monitoring. Literature review also reveals that speed, feed, thrust force, torque, drill diameter and chip thickness have been established as important parameters indicative of drill wear and hence condition of drill. In case of online monitoring, it is not always possible to have a quantitative measure all these parameter and hence it becomes advantageous to describe one or more of these parameters as fuzzy linguistic variables. Therefore the aim of the present work is to develop a fuzzy back propagation neural network which could be trained with large number of drilling experiments conducted at different cutting conditions for future prediction of drill wear while using same types (material compositions) of drill on same types (material compositions) of work piece material.

2 Tool Life Criteria

Tool life is based on the limiting wear land of the flank wear. The criteria recommended by ISO to define the effective tool life for high speed steel tools are (i) catastrophic failure (ii) regularly worn flank wear of 0.3 mm or maximum flank wear of 0.6 mm. One way of determining drill life is to evaluate drill flank wear which can be done directly by

measuring drill flank wear periodically after cutting a predetermined depth of cut in drilling. This method is known as offline monitoring in which drill is removed periodically from machine tool to measure wear.

The maximum flank wear is used as the criterion to characterize the drill condition, and is obtained by measuring the wear at different points on either of the cutting edges as shown in Fig.1, in which 1,2,3,4 are the points on the cutting edges where wear has taken place and measurement is done on these points [1].

3 Fuzzy Back Propagation Neural Network

In fuzzy back propagation neural network, fuzzy input is mapped with crisp output. The fuzzy neuron makes use of left and right (*LR* type) fuzzy number. A triangular type membership function has been used for simplification of architecture and reduction of computational load.

3.1 LR type of fuzzy number

LR type fuzzy number having two function values called left and right (*L* and *R*) which maps with real number within [0,1] and are the decreasing shape function if

$$\begin{aligned} &L(0) = 1, \\ &L(x) < 0, \forall x < 1, \\ &L(1) = 0, L(\infty) = 0 \end{aligned} \tag{1}$$

A fuzzy number *M* is of type *LR* if there exists reference functions *L* (for left), *R* (for right and scalar, $\alpha > 0, \beta > 0$ with

$$\mu_m = \begin{Bmatrix} L(\frac{m-x}{\alpha}), x \le m \\ R(\frac{x-m}{\beta}), x \ge m \end{Bmatrix} \tag{2}$$

Here *m* is called the mean value of *M*, is a real number, and α and β are called left and right spread, respectively. μ_m is the membership function of fuzzy number *M*. So an *LR* type fuzzy number *M* can be expressed as $(m, \alpha, \beta)_{LR}$. If α, β are both zero, the *LR* type function indicates a crisp value.

3.2 Fuzzy neuron

The fuzzy neuron is the basic element of a fuzzy back propagation neural network model. Fig. 2 illustrates the architecture of a fuzzy neuron. Given the input vector

$I = (I_0, I_1, ...I_l)$ and weight vector $W = (W_0, W_1, ...W_l)$, the fuzzy neuron computes the crisp output *O*, given by

$$O = f(NET) = f\left(CE\left(\sum_{i=0}^{l} W_i I_i\right)\right) \quad (3)$$

$I_0 = (1,0,0)$ is the bias value. Here, fuzzy weight summation is

$$net = \sum_{i=0}^{l} W_i I_i \quad (4)$$

The function *CE* is the centroid operation of the triangular fuzzy number, and can be treated as defuzzification operation, which maps fuzzy weight summation value to a crisp value. Thus, if $net = (net_m, net_\alpha, net_\beta)$ is the fuzzy weight summation then function *CE* is given by

$$CE = net_m + 1/3(net_\beta - net_\alpha)$$

The function *f* is the sigmoidal function, which performs nonlinear mapping between input and output is defined as

$$f(NET) = \frac{1}{1 + \exp(-NET)} \quad (5)$$

In the fuzzy neuron, both input vector *I*, and weight vector *W* are represented by a triangular *LR* type fuzzy number. Thus for $I = (I_0, I_1, ...I_l)$ the input component vector I_i is represented by *LR* type fuzzy number $(I_{mi}, I_{\alpha i}, I_{\beta i})$. Similarly for $W = (W_0, W_1, ...W_l)$, the weight vector component W_i is represented as $(W_{mi}, W_{\alpha i}, W_{\beta i})$

3.3 Fuzzy back propagation neural network architecture

Fuzzy back propagation neural network is a three-layered feed forward architecture. The three layers are input layer, hidden layer and output layer. Functioning of fuzzy back propagation proceeds in two stages, namely learning or training and testing.

Fig. 3 shows the *l-m-n* (*l* input neurons, *m* hidden neurons and *n* output neurons) architecture of a fuzzy back propagation neural network model.

Let $I_p = (I_{p1}, I_{p2}, ...I_{pl}), p = 1, 2....N$ be the p^{th} pattern among *N* input patterns with $I_0 = (1,0,0)$ as bias. Here, $I_{pi} = (I_{pmi}, I_{p\alpha i}, I_{p\beta i})$. O_{pi}, O_{pj} and O_{pk} are the i^{th}, j^{th} *and* k^{th} crisp defuzzification output of neuron from input, hidden and output layers,

respectively. W_{ji} and W_{kj} are *LR* type fuzzy connection weights between i^{th} input neuron to j^{th} hidden neuron, and j^{th} hidden neuron to k^{th} output neuron, respectively.

Output from a neuron in the input layer is,

$$O_{pi} = I_{pi}, i = 1, 2.....l \tag{6}$$

Output from a neuron in the hidden layer is,

$$O_{pj} = f(NET_{pj}) = f\left(CE\left(\sum_{i=0}^{l} W_{ji} O_{pi}\right)\right), j = 1, 2.....m \tag{7}$$

Output from a neuron in the output layer is,

$$O_{pk} = f(NET_{pk}) = f\left(CE\left(\sum_{j=0}^{m} W_{kj} O_{pj}\right)\right), k = 1, 2.....n \tag{8}$$

3.4 Learning or training in fuzzy back propagation neural network

Sample mode type of supervised learning has been used in the present case, where, all input-output pattern sets are presented to the neural network one by one, and then interconnection weights are adjusted using average gradient information. During training, the predicted output is compared with the desired output, and the mean square error is calculated. If the mean square error is more than a prescribed limiting value, it is back propagated from output to input, and weights are further modified till the error is within a prescribed limit.

Mean square error, E_p for pattern *p* is defined as

$$E_p = \sum_{i=1}^{n} \frac{1}{2} (D_{pi} - O_{pi})^2 \tag{9}$$

where, D_{pi} is the target output, and O_{pi} is the computed output for the i^{th} pattern.

Weight change at any time *t*, is given by

$$\Delta W(t) = -\eta E_p(t) + \alpha \times \Delta W(t-1) \tag{10}$$

where η is learning rate, and α momentum parameter.

3.5 Testing of fuzzy back propagation neural network

The error on the testing set is monitored during the training process. The testing error will normally decrease during the initial phase of training, as does the training set error. However, when the network begins to over fit the data, the error on the testing set will typically begin to rise. When the testing error starts increasing for a specified number of

iterations, the training is stopped; and the weights and biases at the minimum value of the testing error are returned.

4 Experimental Set-up

In the present work, large number of drilling operation over a wide range of cutting conditions has been performed, and corresponding to each cutting condition progressive flank wear of drill has been measured.

Fig. 4 shows a schematic representation of the experimental set up used in this work. A radial drilling machine (Batliboi Limited, BR618 model) is used for the drilling operation. High-speed steel (HSS) drill of three different diameters (chemical composition and geometrical specification) are listed in Tables 1 (a) and (b) have been used to drill holes on mild steel (refer Tables 2 (a) and (b) for specification and compositions) specimen at different cutting condition. In all the drilling operations performed in the present work, no coolant has been used. Signals from the piezoelectric dynamometer were passed through low pass filter, amplified through charge amplifier (B&K, 2525), and stored in the computer through a data acquisition system (Advantech, PCL 818 HG, 100 kHz sampling rate). For each cutting condition, drilling process was carried out in mild-steel work piece up to 15mm depth of cut and sensor data was captured through the dynamometer, which was stored in the computer through data acquisition system during time of drilling. The data stored in the computer is instantaneous and hence an offline analysis was done to calculate the root mean square (RMS) of the data. In order to check the consistency of the data, initially three different 10mm diameter drill at a given cutting condition has been used and root mean square value of thrust force and torque has been observed in each case. It was found that variation is less than ±10%. After each drilling operation, tool was taken out and flank wear was measured through digital microscope along with Carl-Zeiss software interfacing. After locating the maximum flank wear on either of cutting edges, a grid in micro meter scale is imposed and the maximum depth of flank wear is measured in the vertical direction as per the number of grid division. Photographs of gradual wear build-up process in the drill for three different feed rates are shown in Fig. 5(a)-5(c).

5. Results and Discussion

Drilling operations have been conducted over a wide a range of cutting condition. Spindle speed has been varied in the range 315 *rpm* to 1000 *rpm* in six steps. Feed rate has been varied from 0.13 to 0.71 *mm/rev* in six steps. High speed steel (HSS) drill of three different diameter size of 5*mm*, 7.5*mm* and 10*mm* have been used for drilling hole in a mild steel plates. Various combinations of spindle speed, feed rate and drill diameter have

been used to perform 52 different drilling operations. For each of these conditions, thrust force and torque have been measured using the dynamometer, and the data is stored in the computer through the data acquisition system. Also corresponding to each cutting condition, maximum flank wear has been measured. The results of the experiment are tabulated in Table 3. In this table chip thickness is shown as a fuzzy linguistic variable, which can be medium (M), low (L) or high (H). This is described in details in the section 5.2.

5.1 Effect of important parameters on thrust force and torque

Fig. 6 shows the variation of thrust force with drill diameter for different spindle speeds. It could be observed that for a particular spindle speed, thrust force increases as drill diameter is increased. This is due to the fact that the un-deformed chip thickness increases, as the drill diameter is increased leading to increase in thrust force. This is an established fact known as size effect [1]. It could be observed that for a particular drill diameter thrust force decreases with increasing spindle speed. This is due to fact that increasing spindle, tool chip interface temperature increases and thus the strength of the work material reduces [1] leading to decrease in thrust force. Fig. 7 shows the variation of torque with drill diameter for different spindle speeds. Here it also could be observed that a for a particular spindle speed, torque increases as drill diameter is increased and for a particular drill diameter torque decreases with increasing spindle speed due to the same reason as stated in the case of thrust force.

5.2 Wear prediction by fuzzy back propagation neural network

Fuzzy back propagation neural network architecture, considered in the present work, comprises of six input nodes with the input parameters as spindle speed, feed rate, drill diameter, thrust force, torque and chip thickness. The output parameter of the network is flank wear, and hence the number of neuron in output layer is one. In case of portioning the experimental data into training and testing data different publication [14,15,16,17,18] have been referred .

After shuffling the 52 data set, 37 have been selected at random for training the network, and remaining 15 are used for testing. The normalized data sets are used for training the network. The data sets are normalized in the range of 0.1 to 0.9 using

$$y = 0.1 + 0.8\left(\frac{x - x_{\min}}{x_{\max} - x_{\min}}\right) \qquad (11)$$

where,

x = Actual value,

x_{max} = Maximum value of x,

x_{min} = Minimum value of x,

y = Normalized value corresponding to x.

In the present model, chip thickness is used as a fuzzy input, and spindle speed, feed rate, drill diameter, thrust force and torque are used as crisp input for the fuzzy back propagation neural network. All the crisp data sets are converted into LR type fuzzy number by assigning zero to left and right spread. A triangular membership function has been used to describe chip thickness as fuzzy input parameter. Fuzzy sets of chip thickness are overlapped by the adjacent one by 25% as shown in Fig. 8. In the present work, it is assumed that maximum chip thickness could be 1.2 *mm*, hence fuzzy set of low, medium and high chip thickness is assigned in the range of 0-1.2 *mm*.

Best network architecture (i.e., number of hidden layers, number of neurons in the hidden layers, learning rate and momentum coefficient) has been obtained by trial and error based on mean square error (MSE) in training, testing, and the number of iterations. Large numbers of runs were given for selecting the best architecture and few of these are shown in Table 4. The best network architecture arrived at in the present model is 6-9-1 with learning rate (η)=0.9 and momentum coefficient (α)=0.6. Fig. 9 shows the mean square error in training and testing with number of iteration. It could be observed from the Fig. 10 that flank wear predicted by the present fuzzy neural network is very close to $\pm 10\%$ of the actual values. Most of the values are within the $\pm 5\%$ error band.

6 Conclusions

In the present work, a fuzzy back propagation neural network model has been developed for predicting flank wear of drill in drilling operations by a specific class of drill on a specific work piece. In the present model all the input parameters for the neural network could be either fuzzy or crisp variables, which will provide the crisp output. In this model five parameters are crisp inputs, and one parameter is used as fuzzy input. A triangular membership function has been used to describe the fuzzy parameter. Several tests have been performed in drilling to train and test the fuzzy neural network. A large number of fuzzy neural network architecture have been considered, and the best architecture has been predicted. All the predicted flank wear by the best architecture came out to be very close to the actual values, and most of them lie within $\pm 5\%$ error-band. This present fuzzy neural network model has the potential to be used for the online prediction and control of drill flank wear. Even through the present methodology has been developed for predicting drill wear at any time during drilling operation, it could also be extended for drill life prediction based on limiting drill wear criterion.

References

[1] S.C. Lin, C.J. Ting (1995), Tool wear monitoring in drilling using force signals, **Journal** of Wear 180: 53-60.

[2] S.C. Lin, C.J. Ting (1996), Drill wear monitoring using neural network, International Journal of Machine Tool Manufacturer 36: 465-475.

[3] B.Y. Lee, H.S. Liu, Y.S. Tarng (1998), Modeling and optimization of drilling process, Journal of Material Processing Technology 74: 149-157.

[4] Li Xiaoli, S.K. Tso (1999), Drill wear monitoring based on current signals, Journal Wear 231: 172-178.

[5] C.C. Tsao (2002), Prediction of flank wear of different coated drills for JIS SUS 304 stainless steel using neural network, Journal of Material Processing Technology 123: 354-360.

[6] H.M. Ertunc, K.A. Loparo (2001), A decision fusion algorithm for tool wear condition monitoring in drilling, International Journal of Machine Tool Manufacturer 41: 1347-1362.

[7] I. Abbu-Mahfouz (2003), Drilling wear detection and classification using vibration signals and artificial neural network, International Journal of Machine Tool Manufacturer 43: 707-720.

[8] D. Kim, M. Ramulu (2004), Drilling process optimization for graphite/ bismaleimide-titanium alloy stack, Journal of Composite structures 63: 101-114.

[9] A.K. Singh, S.S. Panda, S.K. Pal, D. Chakraborty, Predicting drill wear using an artificial neural network, International journal of advanced manufacturing technology, Accepted in the press.

[10] X. Li, S. Dong, P.K. Venuvinod (2000), Hybrid learning for tool wear monitoring, International journal of advanced manufacturing technology 16: 303-307.

[11] R.J. Kuo, P.H. Cohen (1999), Multi-sensor integration for online tool wear estimation through radial basis function networks and fuzzy neural network, neural network 12: 355-370.

[12] S.-P. Lo (2002), The application of an ANFIS and Grey system method in turning tool-failure detection, International journal of advanced manufacturing technology 19: 564-572.

[13] K. Hashmi, I.D. Graham, B. Mills (2000), Fuzzy logic based data selection for drilling process, Journal of material processing technology 108: 55-61.

[14] A. Ghasempoor, J. Jeswiet, T.N. Moore (1999), Real time implementation of on-line tool condition monitoring in turning, International journal of machine tool and manufacture 39:1883-1902.

[15] E.O. Ezugwu, D.A. Fadare, J. Bonney, R.B. Da Silva, W.F. sales (2005), Modelling the correlation between cutting and process parameters in high-speed machining of Inconel 718 alloy using an artificial neural network, International journal of machine tool and manufacture 45:1375-1385.

[16] R.J Kuo (2000), Multi-sensor integration for on-line tool wear estimation through artificial neural networks and fuzzy neural network, Engineering application of artificial intelligence 13:249-261.

[17] James A. Freeman, David M. Skapura (2004), Neural Networks Algorithm, Application, and Programming Techniques, Pearson Education.

[18] S. Haykin (2004), Neural Networks a comprehensive foundation, 2nd edition, PHI.

List of Tables

List of Figures

Fig. 7. Variation of average torque with drill diameter at different speeds.

Fig. 8. Membership function

Fig. 9. Variation of mean square error with number of iteration of 6-9-1 architecture (for α =0.6, η =0.9).

Fig. 10. Comparison between experimental values with predicted values of flank wear by 6-9-1 architecture (for α =0.6, η =0.9).

Table 1 HSS drill bit geometry and chemical composition

(a) Geometry of HSS drill bit (long series)

Tool diameter (mm)	Flute length (mm)	Total length (mm)	Point angle(degree)	Helix angle(degree)
5	44.4	76.2	118	30
7.5	60.3	95.2	118	30
10	73	114.3	118	30

Flute	2 flutes
Flute type	parabolic
Shank type	straight cylindrical
Coating any	No

(b) Chemical Composition of HSS drill materials (wt%)

Tungston	Cromium	Vanadium	Cobalt	Molybdenum	Carbon	Hardness
18	4.3	1.1	5	0.65	0.75	290 BHN

Table 2 Mild steel properties and chemical composition

(a) Chemical Composition (wt%)

Carbon	Manganese	Silicon	Sulfur	Phosphorus	Others
0.07	1.1	0.5	0.035	0.025	0.08 Ti 0.07 Zr

(b) Mechanical Properties

Ultimate tensile stress (MN/m^2)	Yield stress (MN/m^2)	Density (Kg/m^3)	Elongation (%)	Vickers Hardness
300	170	7850	42	140

Table 3 : Experimental data for mild steel work-piece

Sl. No.	Drill diameter (mm)	Spindle Speed (m/min)	Feed (mm/rev)	Thrust Force (N)	Torque (N-m)	Chip thickness (mm)	Wear (mm)
1	10	15.71	0.13	3256	0.6	M	0.1
2	7.5	11.78	0.13	667	0.1434	M	0.13
3	5	7.85	0.13	567	0.0958	L	0.08
4	10	15.71	0.18	3298	0.6251	H	0.17
5	7.5	11.78	0.18	692	0.1458	M	0.14
6	5	7.85	0.18	584	0.1012	L	0.04
7	10	15.71	0.25	3789	0.6754	H	0.1
8	7.5	11.78	0.25	1004	0.1722	M	0.3
9	5	7.85	0.25	956	0.1456	L	0.15
10	10	12.56	0.13	3892	0.6276	H	0.12
11	7.5	9.42	0.13	712	0.1524	H	0.09
12	5	6.28	0.13	612	0.0989	L	0.07
13	10	12.56	0.18	3935	0.6472	H	0.07
14	7.5	9.42	0.18	744	0.1565	H	0.13
15	5	6.28	0.18	624	0.1096	L	0.03
16	10	12.56	0.25	4056	0.6821	H	0.09
17	7.5	9.42	0.25	1045	0.173	H	0.08
18	5	6.28	0.25	997	0.1532	M	0.14
19	10	19.78	0.13	2854	0.5165	M	0.04
20	7.5	14.83	0.13	621	0.1125	M	0.17
21	5	9.89	0.13	554	0.0764	L	0.05
22	10	19.78	0.18	2988	0.5762	M	0.11
23	7.5	14.83	0.18	675	0.1215	M	0.07
24	5	9.89	0.18	569	0.0822	L	0.04
25	10	19.78	0.25	3426	0.6111	H	0.1
26	7.5	14.83	0.25	978	0.1654	M	0.2
27	5	9.89	0.25	944	0.1324	L	0.05

28	10	25.11	0.36	2547	0.4895	H	0.0775
29	7.5	18.83	0.36	649	0.1062	M	0.0525
30	5	12.55	0.36	523	0.0624	L	0.045
31	10	25.11	0.5	3021	0.5224	H	0.082
32	7.5	18.83	0.5	696	0.1335	M	0.074
33	5	12.55	0.5	547	0.0864	M	0.0675
34	10	25.11	0.71	3501	0.5761	H	0.094
35	7.5	18.83	0.71	956	0.1524	H	0.088
36	5	12.55	0.71	912	0.1037	M	0.074
37	10	9.88	0.36	4114	0.7156	H	0.096
38	7.5	7.41	0.36	1068	0.1827	H	0.0832
39	5	4.94	0.36	1034	0.1154	M	0.0725
40	10	9.88	0.5	4181	0.7262	H	0.102
41	7.5	7.41	0.5	1112	0.1944	H	0.085
42	5	4.94	0.5	1084	0.1285	M	0.076
43	7.5	7.41	0.71	1434	0.2362	H	0.105
44	5	4.94	0.71	1325	0.1814	M	0.086
45	10	31.36	0.36	2423	0.4451	H	0.068
46	7.5	23.52	0.36	584	0.0647	M	0.044
47	5	15.68	0.36	489	0.0236	M	0.038
48	10	31.36	0.5	2473	0.4632	H	0.074
49	7.5	23.52	0.5	607	0.0738	H	0.062
50	5	15.68	0.5	503	0.0315	M	0.0575
51	7.5	23.52	0.71	921	0.0812	H	0.078
52	5	15.68	0.71	884	0.0457	M	0.065

Table 4: Training error for different neural network architectures

Sl. No.	Network architecture	Momentum coefficient (α)	Learning rate (η)	Mean square error for training	Mean square error for testing	Number of iteration	Maximum Predicted error (%)	Minimum predicted error (%)
1	6-9-1	0.7	0.5	0.000241	0.0003	6965	-12.63	-0.24
2	6-7-1	0.7	0.5	0.00235	0.000465	11188	-21.4	-1.1
3	6-9-1	0.5	0.7	0.00195	0.00023	10375	-14.28	-0.17
4	6-9-1	0.3	0.8	0.00195	0.000235	12505	10.47	0.04
5	6-8-1	0.8	0.3	0.00105	0.000085	18732	-17.05	0.41
6	6-10-1	0.8	0.3	0.0028	0.00039	7005	-17.62	-0.14
7	**6-9-1**	**0.6**	**0.9**	**0.0004**	**0.000115**	**19382**	**9.94**	**-0.04**
8	6-9-1	0.7	0.9	0.00055	0.000215	11101	36.64	-0.06
9	6-6-1	0.7	0.9	0.0012	0.0002	11751	-14.76	0.08
10	6-8-1	0.7	0.9	0.0005	0.00016	12452	34.22	-0.19

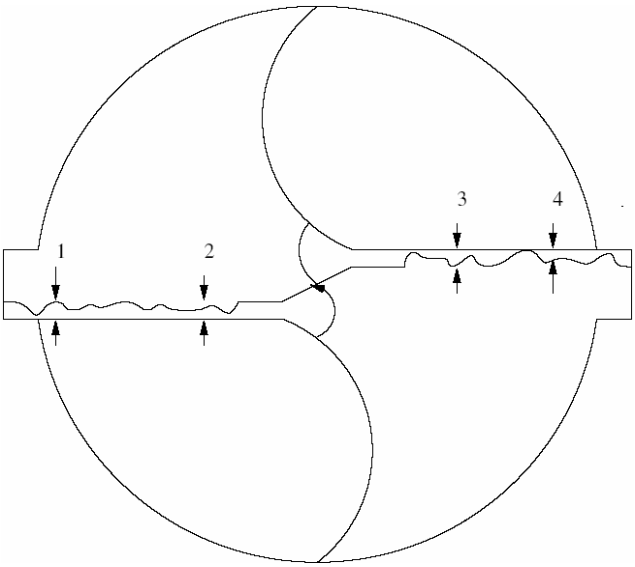

Fig. 1. Flank wear measurement

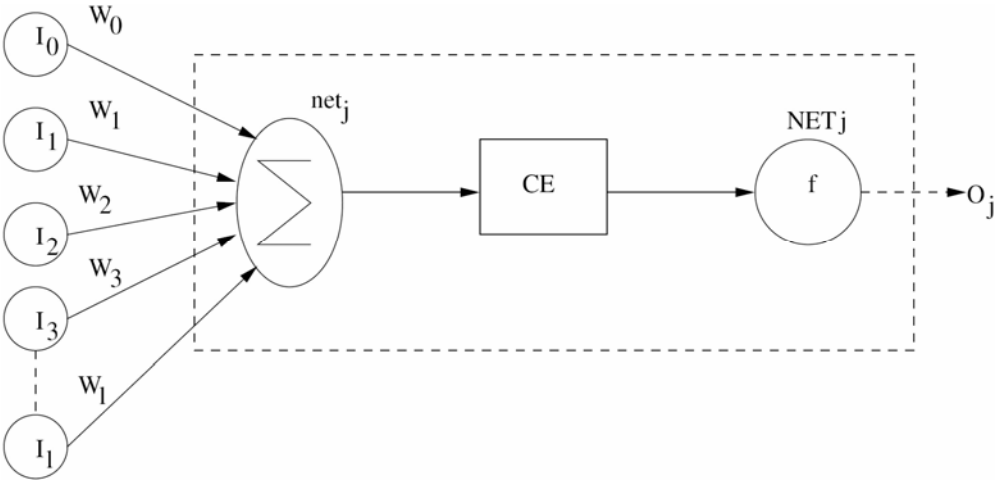

Fig.2. Fuzzy neuron architecture

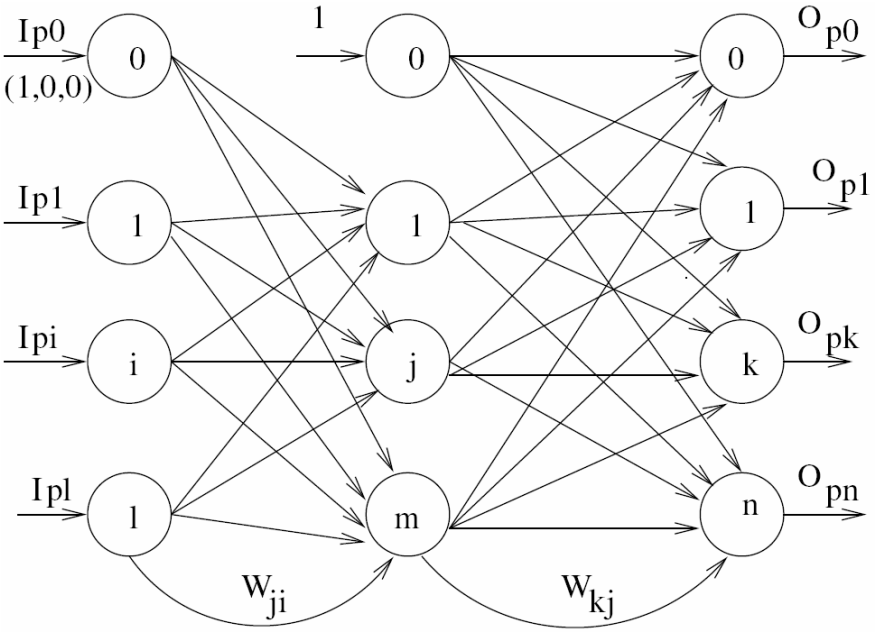

Fig 3. Architecture of fuzzy back propagation

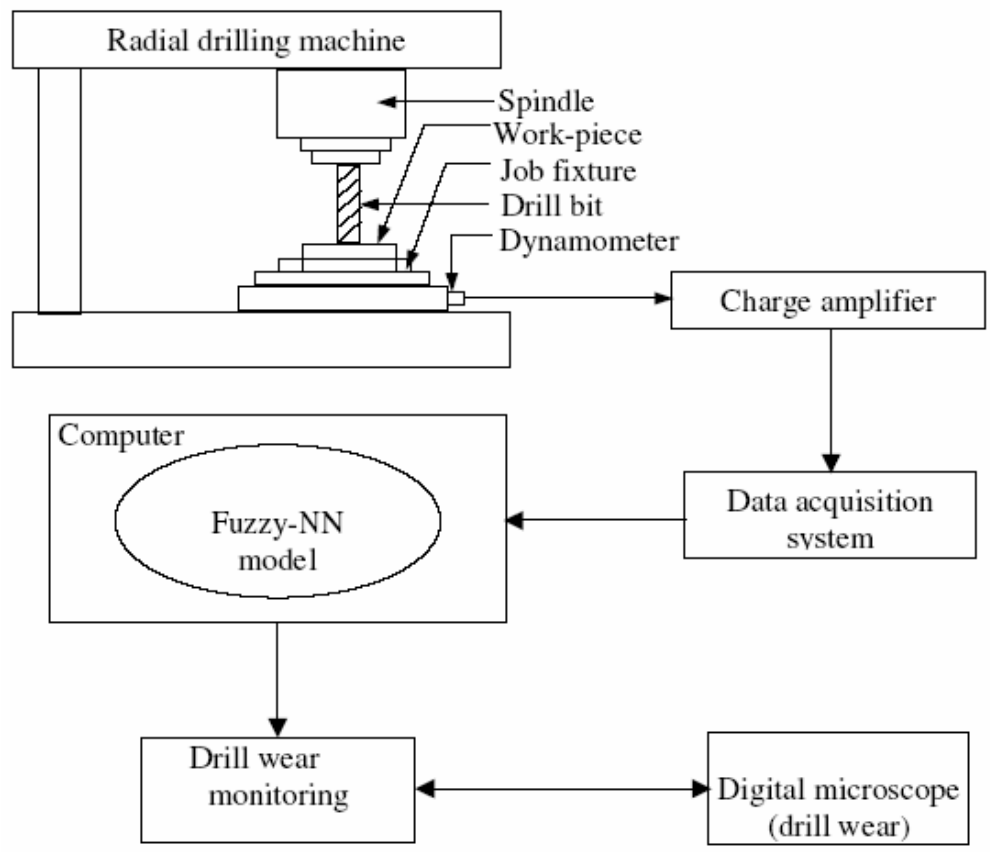

Fig 4. Schematic diagram of experimental set-up

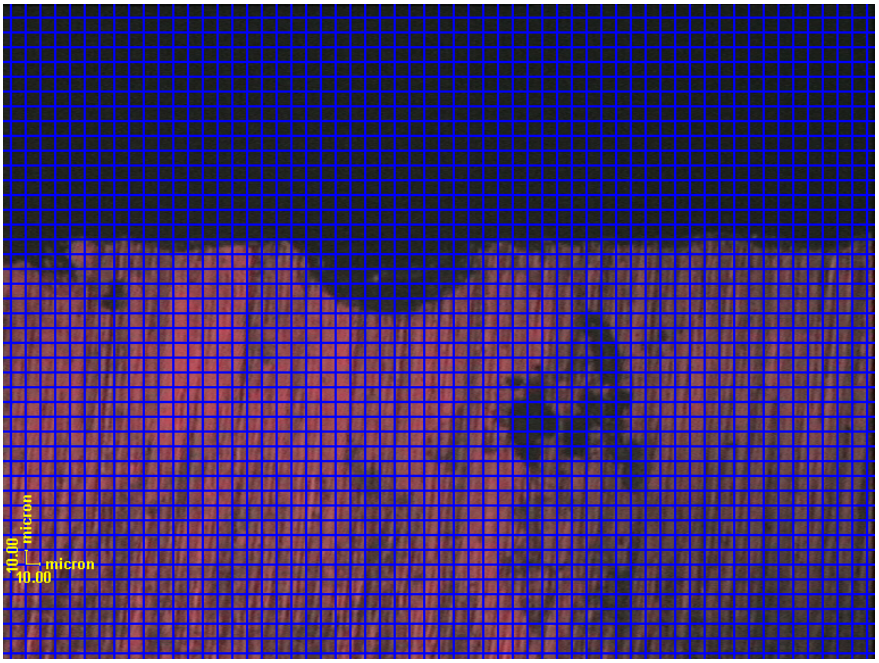

Fig.5 (a) Flank wear at diameter 10mm, spindle speed 19.78m/min and feed rate 0.13mm/rev

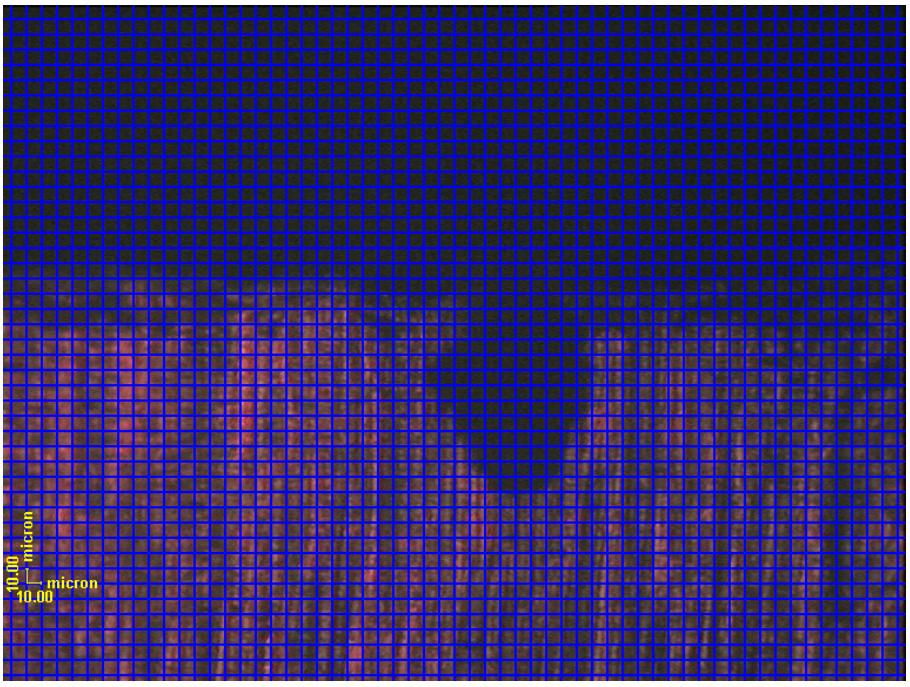

Fig.5 (b) Flank wear at diameter 10mm, spindle speed 19.78m/min and feed rate 0.18mm/rev

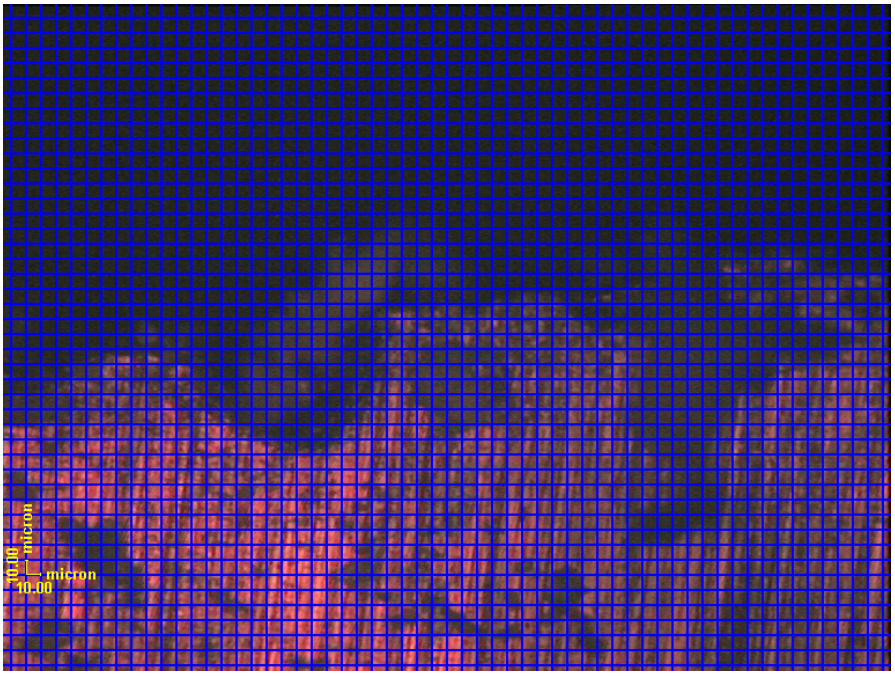

Fig.5 (c) Flank wear at diameter 10mm, spindle speed 19.78m/min and feed rate 0.25mm/rev

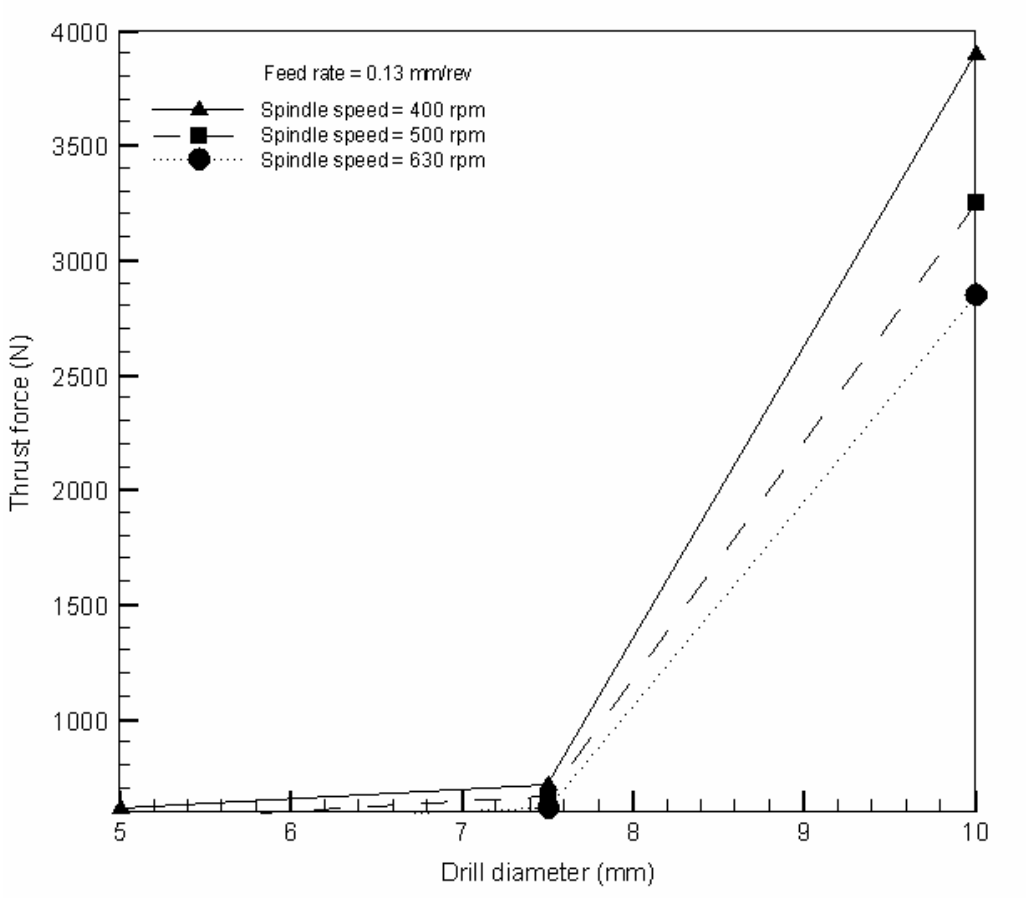

Fig 6. Variation of average thrust force with drill diameter at different speeds

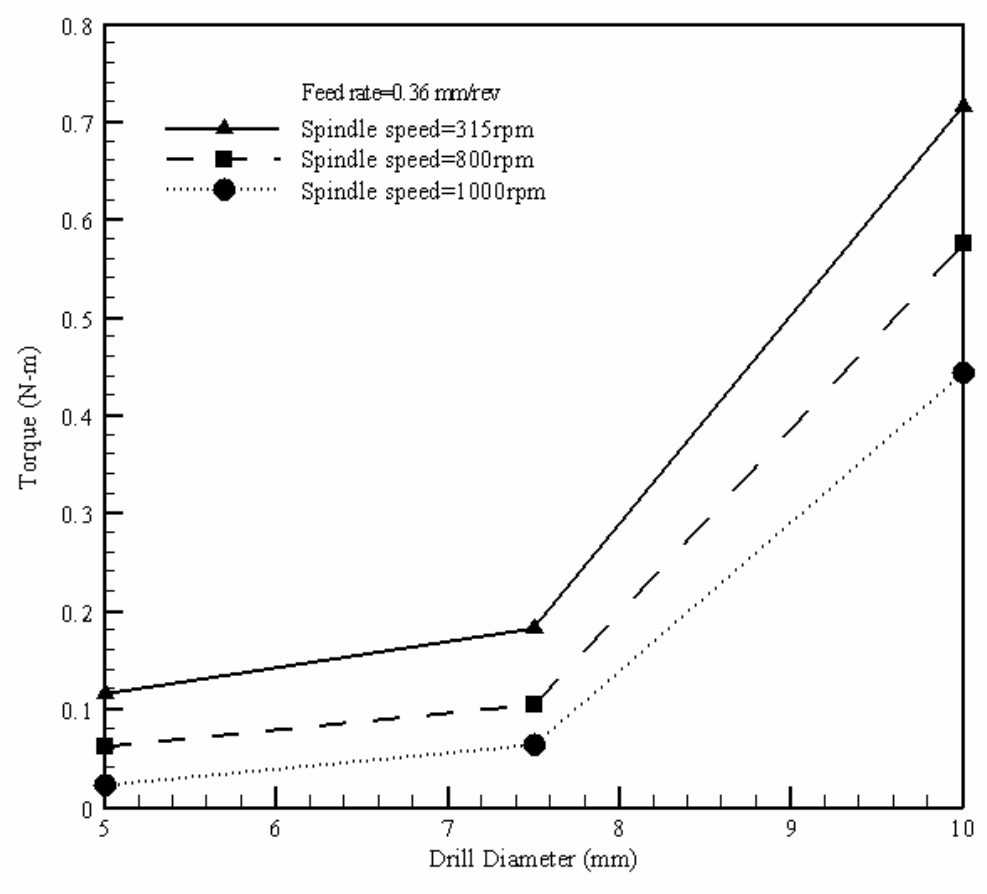

Fig 7. Variation of average torque with drill diameter at different speeds

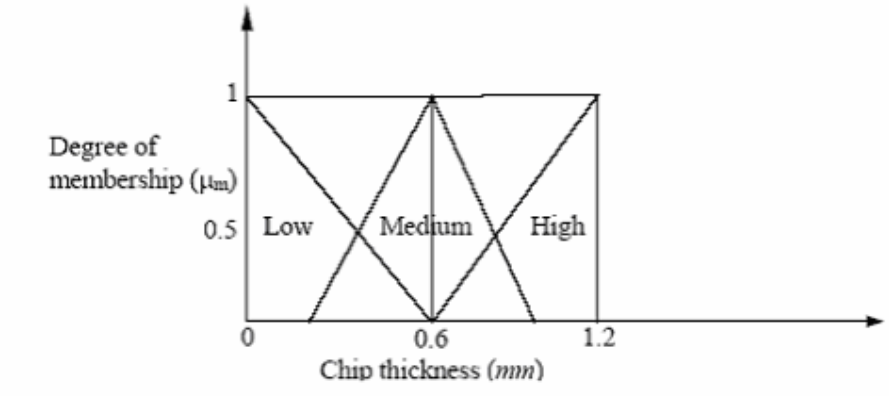

Fig 8. Membership function

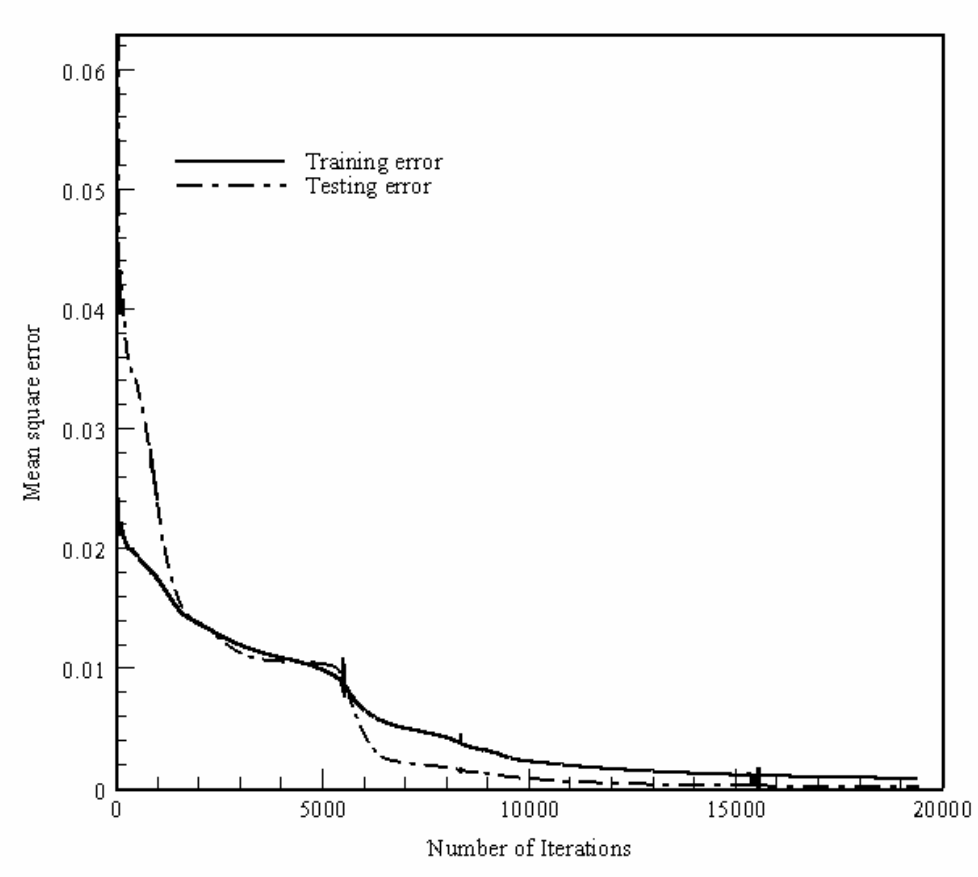

Fig 9. Variation of mean square error with number of iteration of 6-9-1architecture (for $\alpha = 0.6, \eta = 0.9$)

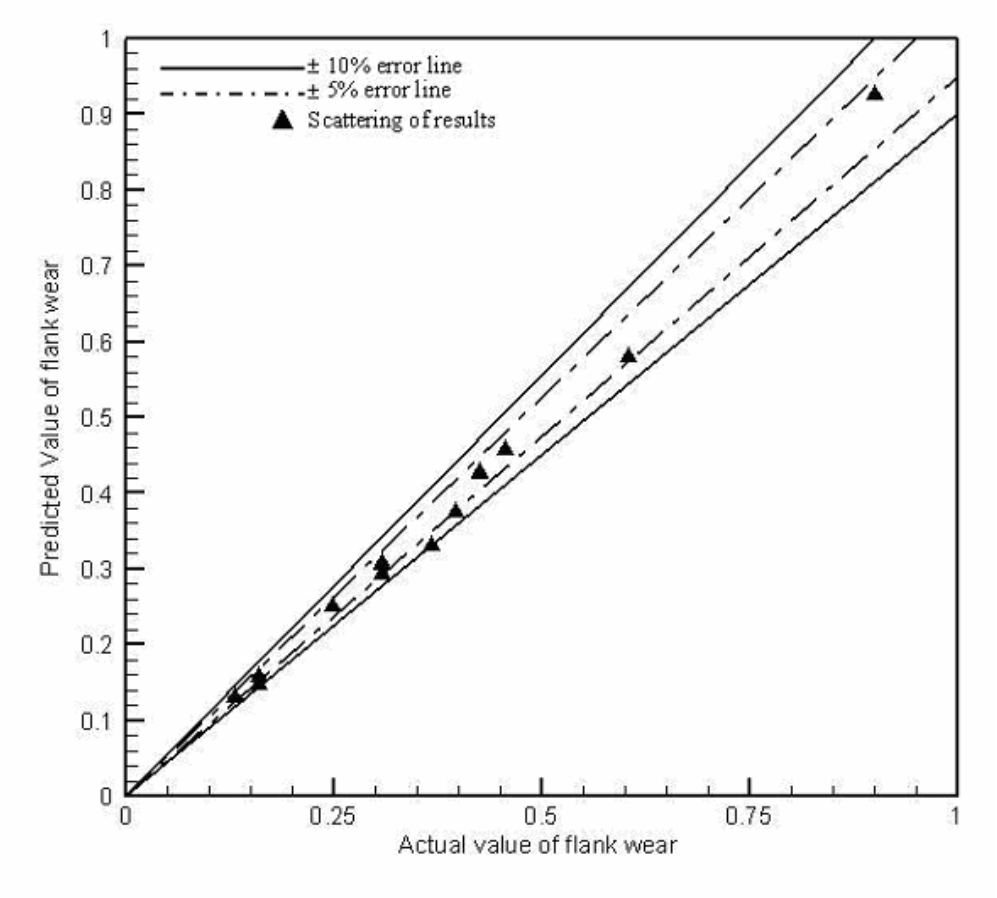

Fig 10. Comparison between experimental values and predicted values of flank wear by 6-9-1 architecture (for $\alpha = 0.6, \eta = 0.9$)